Vrije Universiteit Brussel

Room-temperature versus heating-mediated healing of a Diels-Alder crosslinked polymer network

Diaz, M. M.; Brancart, J.; Van Assche, G.; Van Mele, B.

Published in:
Polymer

DOI:
10.1016/j.polymer.2018.08.026

Publication date:
2018

License:
CC BY-NC-SA

Document Version:
Accepted author manuscript

Link to publication

Citation for published version (APA):
Diaz, M. M., Brancart, J., Van Assche, G., & Van Mele, B. (2018). Room-temperature versus heating-mediated healing of a Diels-Alder crosslinked polymer network. *Polymer*, *153*, 453-463. https://doi.org/10.1016/j.polymer.2018.08.026

Copyright
No part of this publication may be reproduced or transmitted in any form, without the prior written permission of the author(s) or other rights holders to whom publication rights have been transferred, unless permitted by a license attached to the publication (a Creative Commons license or other), or unless exceptions to copyright law apply.

Take down policy
If you believe that this document infringes your copyright or other rights, please contact openaccess@vub.be, with details of the nature of the infringement. We will investigate the claim and if justified, we will take the appropriate steps.

Download date: 09. Apr. 2024

Room-Temperature versus Heating-Mediated Healing of a Diels-Alder Crosslinked Polymer Network

M.M. Diaz[a,1]* (mechasdiaz@gmail.com), J. Brancart[a,1] (joost.brancart@vub.be), G. Van Assche[a] (guy.van.assche@vub.be), B. Van Mele[a] (bvmele@vub.be)

[a]*Department of Materials and Chemistry, Physical Chemistry and Polymer Science (FYSC), Vrije Universiteit Brussel, Pleinlaan 2, B-1050, Brussels, Belgium*

[1]*These authors contributed equally*

**Corresponding author:* mechasdiaz@gmail.com

Abstract

The healing behavior of a dynamically reversible covalent polymer network with a T_g of 3 ºC, based on the reversible Diels-Alder (DA) cycloaddition between furan and maleimide moieties is reported, for both room-temperature and heating-mediated healing. In previous work the dynamic character of the DA cycloaddition reaction in a polymer network was studied, those findings are used to understand its healing ability. The recovery of mechanical properties by intrinsic healing is studied by Dynamic Mechanical Analysis, quantifying the loss in properties due to incurred damage and assessing their recovery with respect to the original material. The DA cycloadduct bonds in the network can be mechanically activated to autonomously heal damage at room temperature if the damage surfaces remain activated. If the damage surfaces are not brought in contact fast enough they reestablish equilibrium (aging) and lose their autonomous healing potential. In the latter case, only heating-mediated healing can occur, reactivating the healing ability. Controlled damage formation and subsequent sealing of the damage of network coatings is monitored by Atomic Force Microscopy and optical microscopy. The repeatability for both mechanical activation, studied by tensile testing, and thermal cycling, studied by Differential Scanning Calorimetry, is reported.

Keywords: Self-healing efficiency, Diels-Alder reaction, dynamic covalent polymer network

1. Introduction

Until recently material systems and structures were designed according to the 'damage prevention' principle, making them stronger to prevent the occurrence of damage and ultimate failure. In the last decade there has been a shift towards the 'damage management' strategy for the design of new, smart material systems that are able to actively and dynamically manage damage instead of only preventing damage in a passive and static

manner [1,2]. Self-healing materials are a class of smart materials that possess the ability to completely or partially “heal” or repair functional properties after damage [3]. Two types of self-healing materials can be distinguished. Extrinsic self-healing materials are based on a healing mechanism that is not inherent to the material. Common examples are the use of microcapsules [4–7], fibers [8] and vascular systems [9–11] to store or transport healing agents. Conversely, intrinsic self-healing materials possess a built-in healing mechanism. The mechanism responsible for the healing action is activated by a trigger [12], such as heat, light and mechanical force. Ideally, the force or stress causing the damage itself would activate the healing action, without the need for an active external intervention. Such systems are referred to as “autonomous” healing systems. This classification is ambiguous since it is possible that under certain conditions a healing system classified as autonomous may not behave autonomous at all. Conversely, material systems that are not generally classified as autonomous may still exhibit healing if environmental triggers, such as heat or light from the sun are present.

For a self-healing material to achieve an efficient recovery of the functional properties after damage, in general, a number of conditions need to be met and several steps can be identified during a healing event. First, the damage formation and/or the associated loss of properties need to be sensed by the smart material system for the healing mechanism to be activated. Second, the created damaged volume needs to be efficiently sealed in order to achieve successful healing. Two complementary mechanisms will aid an efficient filling of the damage volume: (i) sufficient mobility to fill the damage volume; (ii) mechanisms that minimize the damage volume, such as, elastic recovery [12,13] and shape-memory [14,15] that can assist in sealing the damage site by bringing the damage surfaces closer together. Finally, once the damage is sealed, the material properties need to be recovered. In some cases the functional properties are recovered in parallel to the sealing of the damage. In other cases the recovery of the functional properties happens in a separate final step, especially when a considerable degree of mobility is required to cover large damage volumes [16]. The recovery of the functional properties should be fast, but not too fast, to provide enough time to completely seal the damage [17,18].

Reversible covalent bonds are being used to create intrinsic self-healing materials that can theoretically be healed an infinite number of times on the condition that the reversible bonds responsible for the healing action would not be depleted. Several reversible covalent bonds have been used to design self-healing materials, examples of these are ester exchange [19], C=N exchange [20], disulfide exchange [21], radical exchange [22,23], anthracene photodimers [24,25] and the Diels-Alder reaction [26–28]. It has been demonstrated in earlier work how reversible networks based on the Diels-Alder reaction can achieve heating-

mediated healing of microscopic damage for coating applications [13,29] and for the development of various types of self-healing robotic actuators [30–32].

An important requirement for self-healing polymer networks based on reversible covalent bonds to become autonomous, is that the damaging force preferentially breaks the reversible bonds, rather than the irreversible covalent bonds. Equally important is that after the mechanical breaking of the dynamic covalent bonds, these broken bonds are readily available to form new covalent bonds and are not consumed in side reactions. A reversible polymer network based on Diels-Alder covalent bonds using an amorphous bismaleimide and a furan functionalized compound (called F400-ABMI400) was reported [33]. In that work the kinetics and equilibrium thermodynamics of the Diels-Alder reaction were studied and are shown in Table 1. It was concluded from thermodynamics that the reversible σ-bonds formed during the Diels-Alder cycloaddition reaction between furan and maleimide functionalities are much weaker than typical C-C bonds. Thus, this system was proposed as an excellent candidate for autonomous self-healing polymer network applications. In this paper, the design and interpretation of the self-healing experiments is performed taking into account these earlier results.

Table 1. Kinetic and equilibrium parameters for the F400-ABMI400 polymer network [33]

Kinetic parameters	
$\ln A_{DA}$ (kg mol^{-1} s^{-1})	11.7
E_{DA} (kJ mol^{-1})	53.9
$\ln A_{rDA}$ (s^{-1})	28.3
E_{rDA} (kJ mol^{-1})	105.7
Equilibrium thermodynamic parameters	
$\Delta_r H°$ (kJ mol^{-1})	-51.8
$\Delta_r S°$ (J mol^{-1} K^{-1})	-138.0

For the evaluation of this reversible polymer network several aspects need to be taken into consideration. Together with the ‘damage management’ design principle also the methodology to study and characterize this new class of smart materials needs adjusting. Several tests and techniques evaluating the healing efficiency are documented in literature [3,4,7,12]. However, most attention is focused on the recovery of mechanical properties after healing, without a detailed knowledge of the physical, chemical and morphological behavior of the underlying healing mechanism. This issue has been addressed in a review paper

highlighting the importance of the combined use of monitoring and characterization techniques [34].

Multiple definitions to quantify 'healing efficiency' η have been reported in literature. The most common and most intuitive definition is given in Equation 1, relating the functional properties of the damaged or partially healed material $X(t)$ to the initial properties $X(0)$, prior to damage [3,4,12]. It serves as an indicator for relative or normalized properties. The main drawback of this definition is that this so-defined 'healing efficiency' depends on the magnitude of the damage with respect to the initial properties of the material. This leads to misleading interpretation of results, e.g. if the modulus is only reduced by 10 % upon damaging the sample, this 'healing efficiency' starts already at a value of 90 %. It is most useful in the case where failure is studied with complete loss of functionality. The second definition for healing efficiency (Equation 2) can be understood as the recovery of a certain functional property X, expressed as the recovery of a certain degree or level of damage [7]. This definition is less dependent on the magnitude of the damage and allows comparison between materials or systems with different initial properties, as its value goes from 0 % for the initially damaged material to 100 % after complete healing of the damage.

$$\eta = \frac{X(t)}{X(0)} \qquad \text{Equation 1}$$

$$\eta = \frac{X(t) - X_{\text{damage}}}{X(0) - X_{\text{damage}}} \qquad \text{Equation 2}$$

In this paper the combined use of mechanical analysis, microscopy, and thermal analysis techniques is proposed to study the healing behavior and quantification of the healing efficiency of the reversible covalent Diels-Alder network F400-ABMI400 for both room-temperature and heating-mediated self-healing.

2. Materials and Methods

A poly(propylene glycol) bis(2-aminoproyl ether) Jeffamine D series amine hardener with a degree of polymerization n = 6.1 and a molar mass of 430 g mol^{-1} (J400) was supplied by Huntsman. Furfuryl glycidyl ether (FGE, 96 %) was purchased from Sigma Aldrich and stored at 4 °C. Poly(propylene oxide) 400 bismaleimide (ABMI400) with a degree of polymerization n = 6.1 and a molar mass M_n= 613.4 g mol^{-1} was obtained from Specific Polymers and stored under inert atmosphere. All products (Figure 1) were used as received.

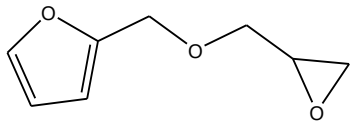

FGE

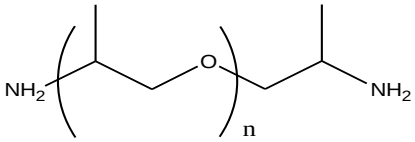

J400 (n = 6.1)

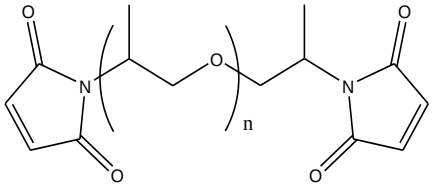

ABMI400 (n = 6.1)

Figure 1 Compounds for the synthesis of the dynamically reversible polymer network F400-ABMI400.

2.1. Synthesis

The thermally reversible covalent polymer network systems were created using a two-step procedure, as described in earlier work [33]. First, the furan functionalized compound F400 was synthesized by mixing a 50% excess of FGE with J400 at room temperature. The mixture was left in a closed flask at 80 °C during 5 days for the irreversible epoxy-amine reaction to take place. Afterwards, the excess of FGE was removed in vacuum at 110 °C for two days and a four-functional furan compound was obtained.

In the second step the tetrafunctional F400 component was mixed and reacted with the ABMI400 bismaleimide in stoichiometric quantities to create a covalent polymer network structure, linked together by means of the Diels Alder active bonds (see Figure 2). Samples for Atomic Force Microscopy and Optical Microscopy where made by casting the mixture on glass slides, and placing a Teflon sheet on top to guarantee a flat surface, samples were left to cure at room temperature for 5 days [33]. Samples with uniform thickness of 1 mm and a flat surface finish were produced for DMA experiments by reacting the mixture between Teflon plates, the formation of the dynamic bonds was sped up by first reacting the monomer mixture at 60 °C for 12 hours and then finishing the reaction at room temperature for 3 more days.

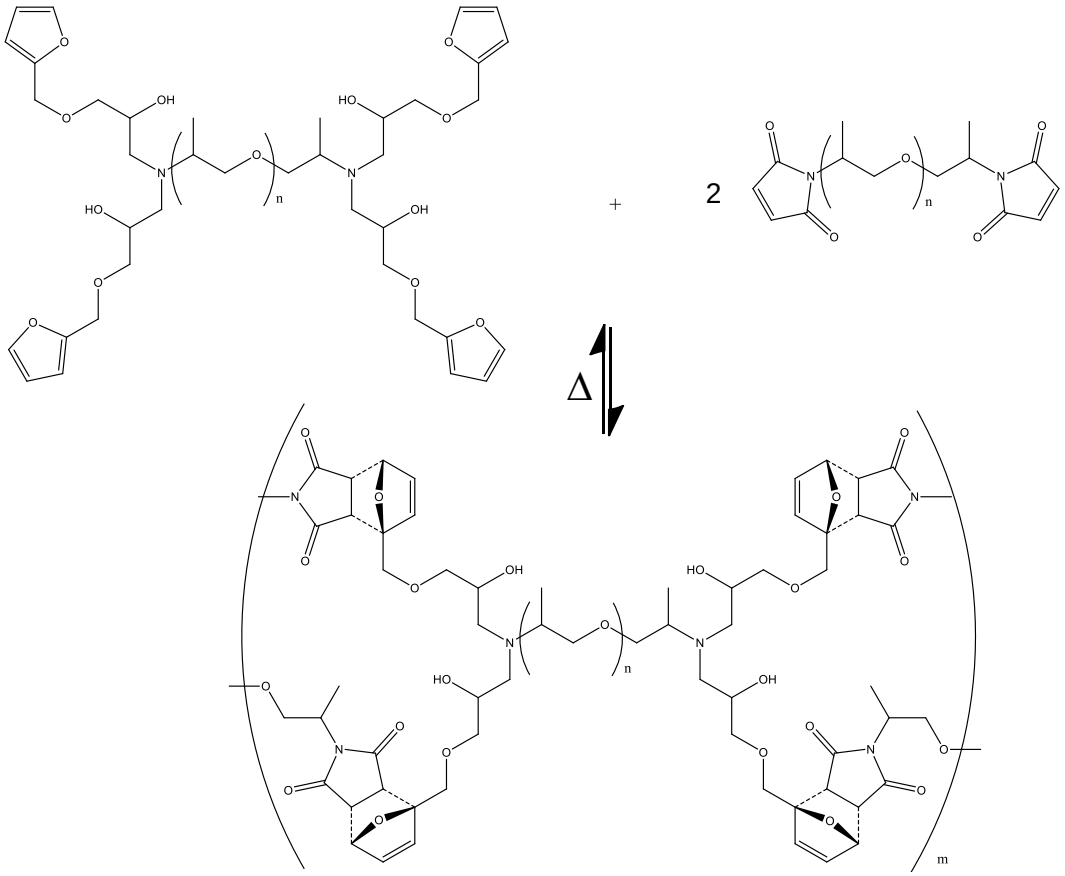

Figure 2 DA and retro DA reaction in the polymer network F400-ABMI400. The reversible covalent bonds are shown with dotted lines.

2.2. Sample preparation and Characterization

Dynamic Mechanical Analysis and Tensile Testing. Mechanical measurements were performed on a TA Instruments Q800 Dynamic Mechanical Analyzer, equipped with a Gas Cooling Accessory (GCA) cooling system. All measurements were performed in tension using the Film/Tension set-up from TA Instruments. Dynamic isothermal measurements were performed at a frequency of 1 Hz and a strain amplitude of 0.1 %. Static stress-strain curves were acquired at different rates ranging from 0.1 to 10 MPa min^{-1}.

Rectangular DMA specimens of about 5.5 mm wide were created from a 1 mm thick sheet of material. The specimens were damaged *in-situ*, still mounted in the DMA set-up, using a scalpel blade. Different types of damage were considered, always applied in the cross-section of the sample specimen. The tensile testing specimens were stored at a temperature of 30 °C to ensure the same thermal and chemical equilibrium for all samples. Still, the mechanical properties vary by about 10 % due to the experimental conditions (clamping effects, the measuring conditions …) and due to small temperature fluctuations during testing, resulting in changes in the reaction equilibrium and the subsequent mechanical properties. In addition, the reference temperature of 30 °C is at the upper end of the glass transition region of the

network F400-ABMI400, increasing the temperature sensitivity of the mechanical properties (viscoelastic contribution instead of pure entropy-elastic behavior).

***Atomic Force Microscopy*.** AFM measurements were performed using an Asylum Research MFP-3DTM AFM equipped with an Olympus AC160TS-E2 AFM tip for imaging (Tapping Mode) and nanolithography (calibrated spring constant of 35.60 N m^{-1}). The samples were given in-situ temperature treatments inside the AFM, using the Asylum Research HeaterCooler stage that allows heating up to 120 °C and cooling to - 20 °C at rates up to 120 °C min^{-1}. All AFM topography measurements were carried out at 20 °C.

***Optical Microscopy*.** A Byomic BYO ST340 (7x-45x) stereomicroscope was used, equipped with a Bresser MicroCAM 3.0 MP camera and a Mettler Toledo FP82HT hot stage to allow in-situ heating of the samples. The samples for optical microscopy were cast onto glass slides and were examined in transmission mode.

***Differential Scanning Calorimetry*.** The reversibility/repeatability of the DA reaction was evaluated by differential scanning calorimetry (DSC) in a TA Instruments Discovery DSC. The procedure involved heating a sample prepared at room temperature (at equilibrium) to 120 °C for 10 min to reach the new equilibrium condition. Afterwards, the sample was cooled at 20 °C min^{-1} to 50 °C and the reformation of the network was followed at this temperature in isothermal conditions during one hour. Ten cycles of this protocol were performed on the same sample to study the repeatability of the thermal activation.

3. Results

3.1. Dynamic character of the reversible Diels-Alder cycloadduct bonds

In previous work [33], the Diels-Alder kinetics and thermodynamics have been thoroughly investigated for the F400-ABMI400 network (Table 1). The dynamic character of the reversible Diels-Alder reaction can be understood by means of two time constants: the relaxation time τ_{DA} (Equation 3) and the cycloadduct lifetime τ_{rDA} (Equation 4). The kinetics of the forward and reverse Diels-Alder reactions increase with temperature, resulting in a decrease in the values of the time constants as shown in Figure 3. The relaxation time τ_{DA} is linked to the time necessary to restore the reaction equilibrium in the case of an off-equilibrium situation. This off-equilibrium situation exists in many cases, such as during the production process, after suddenly heating or cooling the material at high heating or cooling rates or when the reversible bonds are broken by mechanical force. In order for the dynamic reversible character of the Diels-Alder reaction to be practically useful for self-healing applications, the time needed to close or seal damage should be much smaller than the relaxation towards reaction equilibrium.

The cycloadduct lifetime τ_{rDA} is the time an adduct bond is persisting at equilibrium before cleavage and gives an idea about the dynamic character of the bonds at a certain temperature. Heating-mediated healing is based on the decrease in the adduct lifetime and the increase in the dynamics of the Diels-Alder reaction with increasing temperature. The flow behavior of the reversible network at elevated temperature can be explained accordingly (see [33]) which is linked to the sealing ability to close a gap between surfaces after damage (see § 3.4).

$$\tau_{\mathrm{DA}} = \frac{1}{k_{\mathrm{DA}}([\mathrm{F}]_{\mathrm{e}} + [\mathrm{M}]_{\mathrm{e}}) + k_{\mathrm{rDA}}} = \frac{1}{2k_{\mathrm{DA}}[\mathrm{F}]_{\mathrm{e}} + k_{\mathrm{rDA}}} \qquad \text{Equation 3}$$

$$\tau_{\mathrm{rDA}} = \frac{[\mathrm{DA}]_{\mathrm{e}}}{k_{\mathrm{rDA}}[\mathrm{DA}]_{\mathrm{e}}} = \frac{1}{k_{\mathrm{rDA}}} \qquad \text{Equation 4}$$

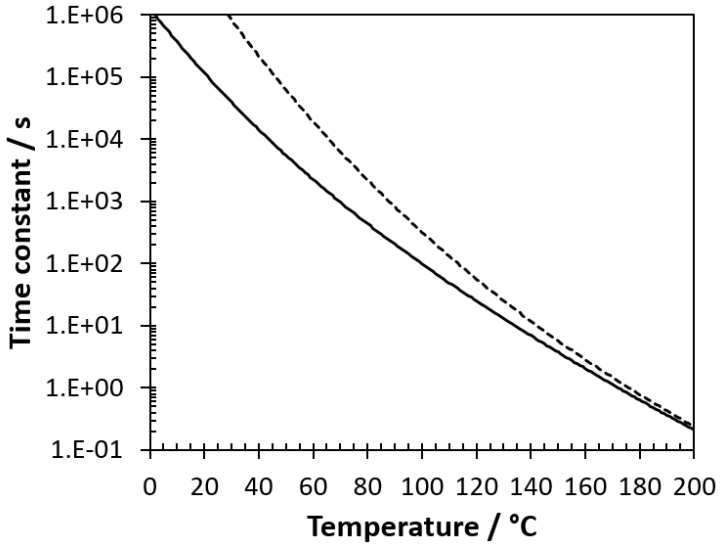

Figure 3 The relaxation time τ_{DA} (solid line) for the reversible Diels-Alder equilibrium and the cycloadduct lifetime τ_{rDA} (dashed line).

3.2. Room-temperature healing of fresh damage surfaces in bulk

The thermal reversibility of the network forming reaction (gelation and de-gelation) was reported for a number of different polymer networks based on four functional furan compounds, reversibly cross-linked using crystalline [29,35] and aliphatic bismaleimides [33]. This reversible network formation was then used to develop self-healing materials for various applications, using heating-mediated healing [13,29-32]. In current work the emphasis is on the restoration of the mechanical properties of the reversible polymer network systems, without the need of heat as an external trigger.

In the scope of the evaluation of the self-healing ability of the F400-ABMI400 system at room temperature, the recovery of the mechanical properties was assessed using DMA. Different types and magnitudes of damage were considered. Figure 4 shows the different types of damage considered in this work. Horizontal incisions were made into rectangular tensile testing specimens, either leaving the two sides (a) or one side (b) of the specimen attached. In addition, the complete failure of a tensile testing specimen was studied (c), either by cutting the entire cross-section of the specimen or by loading the specimen until failure. The location of the damage and the magnitude of the damage will have a strong influence on the degree to which the mechanical tensile properties are lost. An incision damaging 50 % of the cross-section leaving two sides attached will result in a much smaller loss of mechanical properties than an incision made from the side, only leaving one side attached.

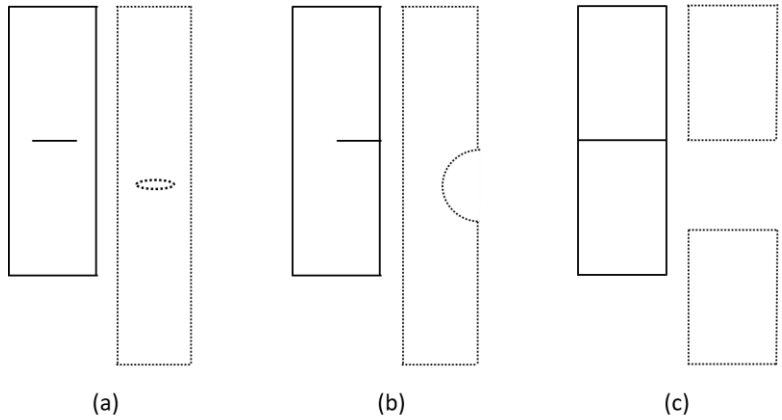

Figure 4 Damage types: (a) incision in the middle of the specimen, (b) incision from one side of the specimen and (c) failure over the entire cross-section. Damage types are shown in relaxed (solid contours) and strained (dotted contours) states.

Sample 1 was damaged in the middle, leaving the sides of the sample attached (Figure 4(a)). A horizontal cut was made using a razor blade, severing the cross-section of the specimen for 40 %, resulting in a 12 % loss of the storage modulus in tension E' (measured at 1 Hz and 0.1 % strain) and a decrease of 16 % of the Young's modulus E (measured at 0.1 MPa min^{-1} and calculated at 1 % strain). All measurements were performed at a reference temperature of 30 °C to ensure that the material is always at thermal and chemical equilibrium at the same temperature, allowing comparison of the properties prior to damage, after damage and during healing. The damaged surfaces of the sample specimen were immediately brought back in contact under mild pressure and allowed to heal for certain amounts of time inside the DMA. After healing, the mechanical properties of the specimen were measured. The results are presented in Figure 5 (left), showing the evolution of the storage and Young's moduli as a function of the healing time. The storage modulus recovers quickly to the original value. In

the first 30 min 75 % of the loss is recovered. The healing efficiency is calculated based on Equation 2, allowing a more reliable physical interpretation than the more common definition of healing efficiency in Equation 1. After 3 hours the storage modulus reaches its original value. The Young's modulus takes longer to recover. After 30 min about 51 % is recovered. The observed differences in recovery behavior between dynamic storage and Young's moduli are due to the different strain levels and measuring conditions in general (dynamic vs. static mode). In dynamic measurements a small oscillatory displacement is applied to the sample, whereas, in stress-strain measurements a continuous increasing load is applied. It was noted that the activated damage surfaces showed initial stickiness, quickly recovering the broken bonds locally. The small oscillatory strain of 0.1 % is expected to be less destructive than the strain levels of several % for the stress-strain curves from which the Young's modulus is calculated (at 1 % strain), whilst also being less sensitive for macroscopic damage and healing evaluation, resulting in higher recovery efficiencies and rates than the static tensile testing method. It should thus be concluded that the stress-strain measurements provide a stricter evaluation of the recovery efficiencies and rates of the mechanical properties and longer healing times are required to recover the mechanical properties for larger deformations.

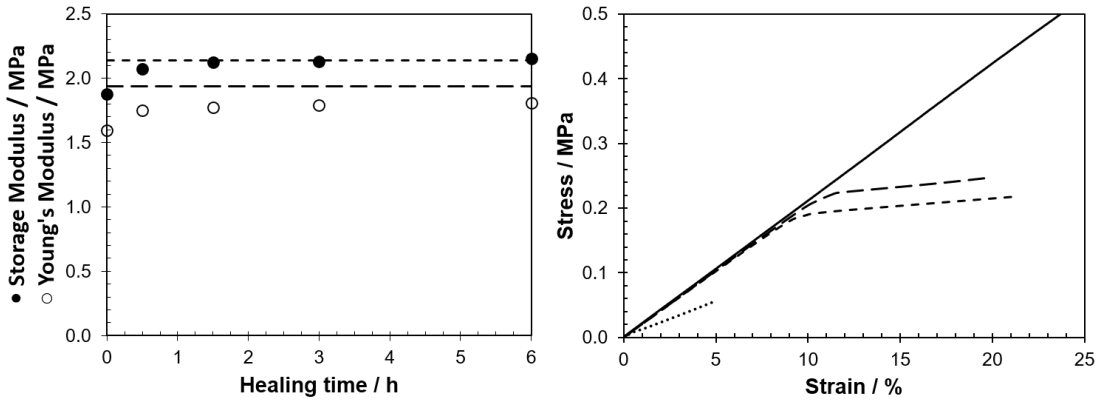

Figure 5 (left) Storage modulus in tension (solid markers, at 1 Hz and 0.1 % strain) and Young's modulus (empty markers, at 1 % strain and 0.1 MPa min^{-1}) during healing of Sample 1 at a reference temperature of 30 °C. The recovery of properties (markers) is compared to the initial properties (horizontal short (E') and long (E) dashed lines) as a function of the healing time. (right) Stress-strain curves of Sample 2 prior to damage (solid line), after damage (dotted line) and after two consecutive healing cycles of 48 h (long dashed line) and 45 h (short dashed line), measured at 0.1 MPa min^{-1}.

Sample 2 was cut horizontally from one side (Figure 4(b)), severing about 80 % of the cross-section, resulting in a 50 % reduction of the Young's modulus. Figure 5 (right) shows the

stress-strain curves of the undamaged (solid line) and damaged (dotted line) specimen. Right after the damaged properties were measured, the damage surfaces were brought into contact and the sample was allowed to heal for 48 h at 30 °C. The stress-strain curve of the healed sample (long dashed line) shows that at strains up to 12 % the curve follows the curve of the undamaged sample. At a load of 0.22 MPa the scar of the damage opened up again (rupturing) and the measurement was stopped. A subsequent healing cycle of 45 h results in similar behavior, recovering the load-displacement properties of the original material until 10 % strain and a load of 0.19 MPa where the scar ruptures again.

These observations of self-healing behavior of the polymer network F400-ABMI400 at room temperature, as shown in Figure 5, can be explained assuming that the reversible covalent Diels-Alder bonds between the furan and maleimide moieties are weaker than the irreversible covalent bonds inside the polymer chains, as was concluded from thermodynamics in [33]. When a force is exerted onto the polymer chains the reversible bonds will break preferentially, creating free furan and maleimide moieties (mechanical activation). These free reactive groups are readily available at the damage surfaces. When the damage surfaces are brought back into contact the furan and maleimide groups at the surfaces react with each other to create new bonds, replacing the broken bonds and repairing the damage.

3.2.1 Repeatability of room-temperature healing

Figure 6 shows the results of Sample 3 that was tested until failure at 10 MPa min^{-1}. Immediately after failure, the damaged surfaces were brought back into contact (see damage condition of Figure (c)) and were allowed to heal for 4 days at 30 °C, after which the sample was tested again until failure. At 30 °C the relaxation time τ_{DA} (Equation 3, solid line in Figure 3) for the Diels-Alder equilibrium is of the order of 4 10^4 s or approximately 12 hours [33], meaning that after 4 days at 30 °C the equilibrium should have been restored for 99.97 % (8 times the relaxation time). Seven consecutive healing cycles show excellent repeatability of the healing ability at room temperature. The repeatable self-healing of the F400-ABMI400 polymer network at room temperature, quantified in Figure 6, is demonstrated in the snapshots of Video 1 (electronic version, see link). The images show how a tensile testing specimen was cut into two pieces by a scalpel knife (images A through C). Immediately after the sample was cut the pieces were brought back into contact at room temperature (images D through F). Without the need to increase the temperature, the two pieces reconnect very well, even under the application of a small strain (image G). The application of excess force on the sample results in the failure of the newly formed bonds at the scar of the previous damage (image H). The two pieces are reconnected a second time

(image I), demonstrating the repeatability of the mechanical activation at room temperature. The recovery of the storage modulus after complete failure amounts between 87 and 98 % for the different healing cycles (see Figure 6 (right)). It can be concluded that indeed the dynamically reversible bonds are broken preferentially, allowing excellent recovery of the mechanical properties for multiple times.

However, it should also be noted that the mechanical properties are only recovered until a certain critical load at which the scar of the damage tends to rupture again. In this case the critical rupture stress was about 40 % of the stress at break of the original specimen, while 50 % of the strain at break could be reached. If the healing efficiency is evaluated by comparison of the toughness of the test specimen, calculated by integration of the stress-strain curves relative to the test bar before damage, these toughness efficiencies are much lower than the ones calculated from the storage moduli (values of maximum 23 % after the first healing cycle, see Figure 6 (right)). The stress and strain at break are limited due to the limited healing time of about 4 days for each cycle. The healing times used in this study are sufficiently long to reestablish the chemical equilibrium state at 30 °C, creating bonds across the damage surfaces as the surfaces are brought back into contact. However, the healing efficiency might be limited by topological network effects. Defects and stresses may remain at the scar of the damage where the surfaces are not brought into good contact, resulting in a quicker stress build-up and earlier failure of the sample specimen. Furan and maleimide groups, resulting from the mechanical activation of cycloadduct bonds, deeper inside the material or at voids between the damage surfaces will react to neighboring groups and will not create new bonds across the damage, giving rise to crosslink density fluctuations in the zone of damage. These remaining differences in crosslink density at the damage scar require much longer times to vanish, equaling several times the lifetime of the cycloadduct bonds τ_{rDA} which is about $8\ 10^5$ s or 222 hours at 30 °C. Longer healing times will probably result in higher toughness efficiencies by network rearrangements. Stress relaxation dynamics for adaptive covalent networks are highlighted in [36].

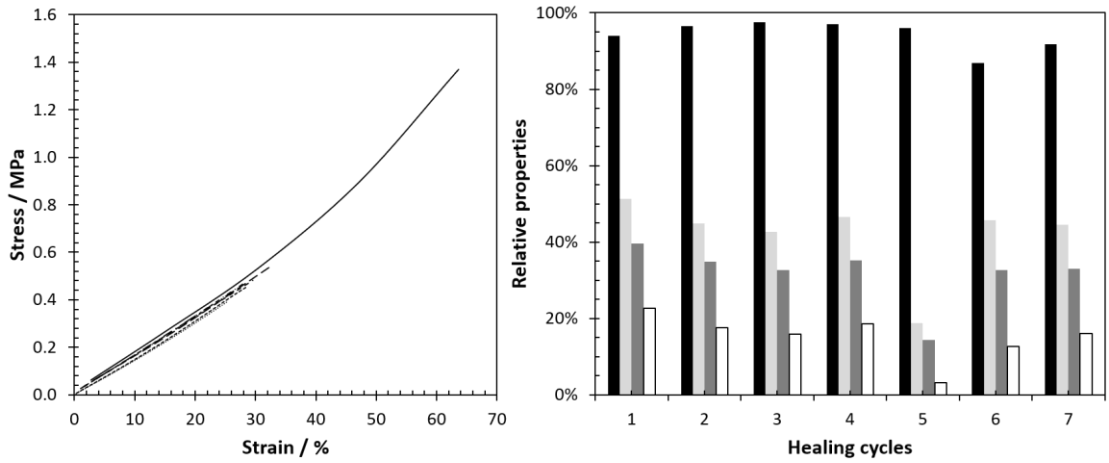

Figure 6 (left) Stress-strain curves of Sample 3 prior to damage (solid line) and after consecutive healing cycles of several days (dotted and dashed lines), until fracture of the tensile testing specimen (10 MPa min^{-1}). (right) Young's modulus (black), strain at break (light grey), stress at break (dark grey) and tensile toughness (empty bars), relative to the pristine material properties, for consecutive healing cycles.

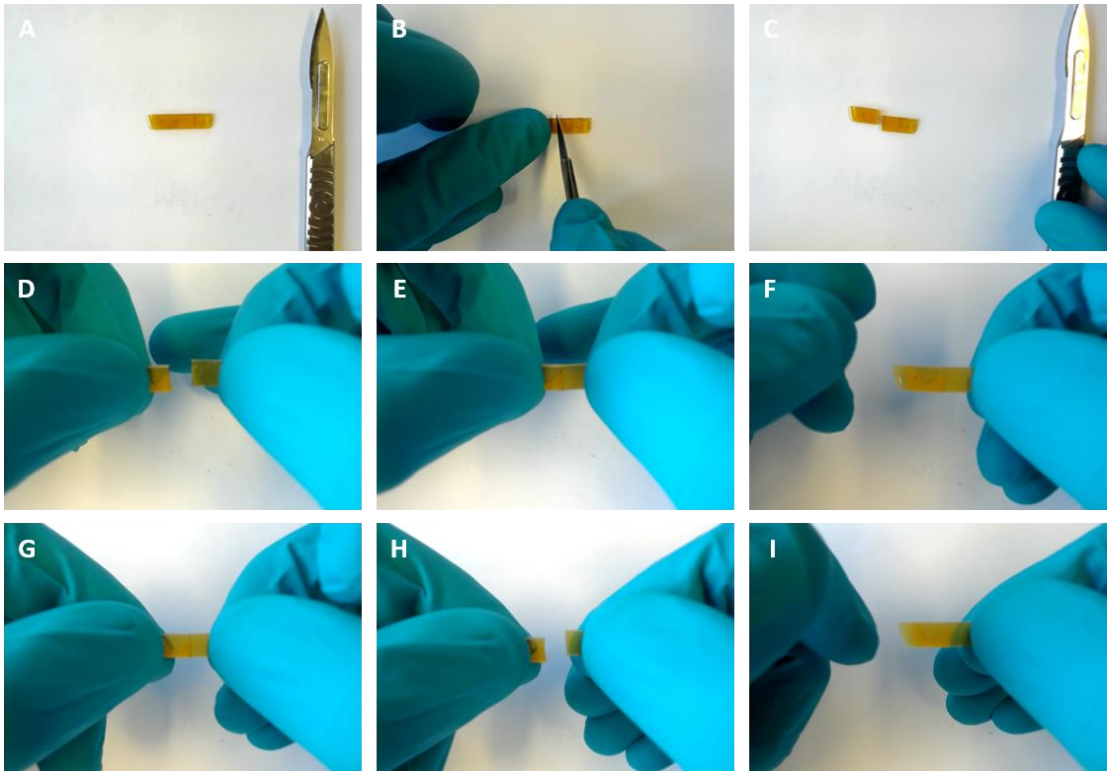

Video 1 Demonstration of the self-healing property of the F400-ABMI400 polymer network at room temperature [LINK].

3.2.2 General requirements for room-temperature healing

The requirements, together with certain limitations, to create the ability to autonomously heal damage at the *same temperature* as the damage occurred (in this case room temperature) can be summarized as follows:

1. A sufficiently large amount of reactive furan and maleimide groups needs to be available to react via the DA reaction across the damage surfaces. This excess of functional groups (against the equilibrium condition at room temperature) is created by preferential mechanical activation and bond rupture of the weaker reversible covalent Diels-Alder bonds between furan and maleimide moieties. A higher local concentration results in faster reaction kinetics of the forward bond-forming reaction and more efficient bond formation across the damage surfaces.
2. The contact between the damage surfaces needs to be made in a sufficiently short time interval for the free reactive groups to be able to react and repair the damage. The time to close the damage ($t_{closure}$) should be sufficiently shorter than the relaxation time constant of the equilibrium reaction ($t_{closure} < \tau_{DA}$) to prevent restoration of equilibrium by consuming the excess of furan and maleimide groups at each damage surface, i.e. fresh damage surfaces should be available and aging of damage surfaces after mechanical activation should be avoided (see also discussion of Figure 7 (left) in § 3.3).
3. A good contact needs to be made and maintained between the damage surfaces to guarantee effective repair of damage and recovery of mechanical properties. The size, geometry and location of the damage will be crucial for the healing efficiency, especially for macroscopically damaged samples (see Figure 4). The gap between damage surfaces can be closed by applying mechanical stress (mechanical sealing) or by heating (flow-induced thermal sealing). The larger the damage volume the higher the 'mobility' needed to efficiently close the damage. Additional mechanisms such as elastic recovery and shape-memory aid the healing action by bringing the damage surfaces closer together [37,38]. In addition, scratches at the surface of a coating and cracks inside the bulk of the material will require a different sealing mechanism and level of mobility to seal the damage volumes (see further discussion in § 3.3.1).
4. The mobility of the polymer chains at the surfaces needs to be high enough for the reactive groups of the broken chains to find a new reaction partner and to create bonds across the damage area. Restrictions to the mobility of the chains, such as vitrification at or below the T_g of the network, will impede or at least substantially slow down the healing action. For this ABMI400-F400 network this is not an issue given that the self-healing experiments are being performed at room temperature while T_g of the network is 3 ºC in these conditions.

3.3. Heating-mediated healing of aged damage surfaces in bulk

A fresh tensile testing specimen of the F400-ABMI400 network (Sample 4, Figure 7) was damaged from the side reducing 60 % of the cross-section (see Figure 4(b)), resulting in a

loss of properties of about 50 %. The freshly cut surfaces were kept apart under mild tension for 12 h (allowing aging of the separate damage surfaces towards equilibrium). Afterwards, the aged surfaces were brought into contact again under minimal pressure in order to heal at 30 °C. The evolution of the storage modulus after aging is shown in Figure 7 (left) as a function of the healing time (24 h). The aged surfaces do no longer show the ability to heal the damage at 30 °C on the time scale tested. When the damage surfaces are kept apart for 12 h, the furan and maleimide functions react locally, reestablishing the equilibrium at both surfaces separately. The aging time of 12 h equals the relaxation time τ_{DA} at that temperature, meaning that the off-equilibrium state at the damage surfaces has recovered for 63 %. The healing efficiency for the room-temperature healing of these aged surfaces still reaches up to 10 % after 24 h (Figure 7 (left)). Without sufficient furan and maleimide groups available to react at the surfaces the damage could still heal very slowly, depending on the dynamically reversible character of the bonds at the actual temperature. At 30 ºC, however, the lifetime of the reversible bonds τ_{rDA} (Equation 4, dashed line in Figure 3) is in the range of 8 10^5 s, which is approximately 222 hours [33], meaning that the equilibrium network at 30 ºC is not really dynamic. Considering this adduct lifetime τ_{rDA} complete healing of aged surfaces cannot be achieved within a reasonable and practically acceptable time frame.

In previous work, thermally reversible polymer network systems were heated to higher temperatures (e.g. 80 °C) to create the necessary mobility to heal microscopic damage in coatings [13,29] or macroscopic damage in robotic actuators [30–32].

In a similar way, to be able to heal the aged damage surfaces of Sample 4, the damaged and aged specimen was heated to 80 °C for 4 h while keeping the cut surfaces apart in the DMA set-up. *After* this heating step, the heat-treated damage surfaces were brought into contact again under minimal pressure and the sample was allowed to recover at 30 °C for several hours. Increase of temperature as an external trigger results in an increase of the kinetics of both forward and reverse reactions and a subsequent decrease in the relaxation time and adduct lifetime (Figure 3). More free furan and maleimide groups are formed as the equilibrium shifts to the breaking of the adduct bonds, which are then available to form new covalent bonds to repair the damage at ambient conditions. ~~In addition, as the equilibrium shifts and the crosslink density decreases, more mobility is created to ease the sealing of the damage.~~ After the heat treatment for 4h at 80 °C equilibrium is reached at 80 °C at both separated damage surfaces (see data of Figure 3). However, the F400-ABMI400 network system goes out of equilibrium in the cooling step from 80 °C to 30 °C because the kinetics are too slow to follow the temperature decrease at normal cooling rates (see Figure 4 in [33]). In this case the time to cool and close the heat-treated damage is sufficiently short to prevent immediate restoration of equilibrium at 30 °C (see requirement 2. of § 3.2.2), i.e. ‘fresh’

damage surfaces are recreated by the heat treatment with an excess of free furan and maleimide groups (see requirement 1. of § 3.2.2), and heating-mediated healing of aged damage surfaces can occur as illustrated in Figure 7 (right).

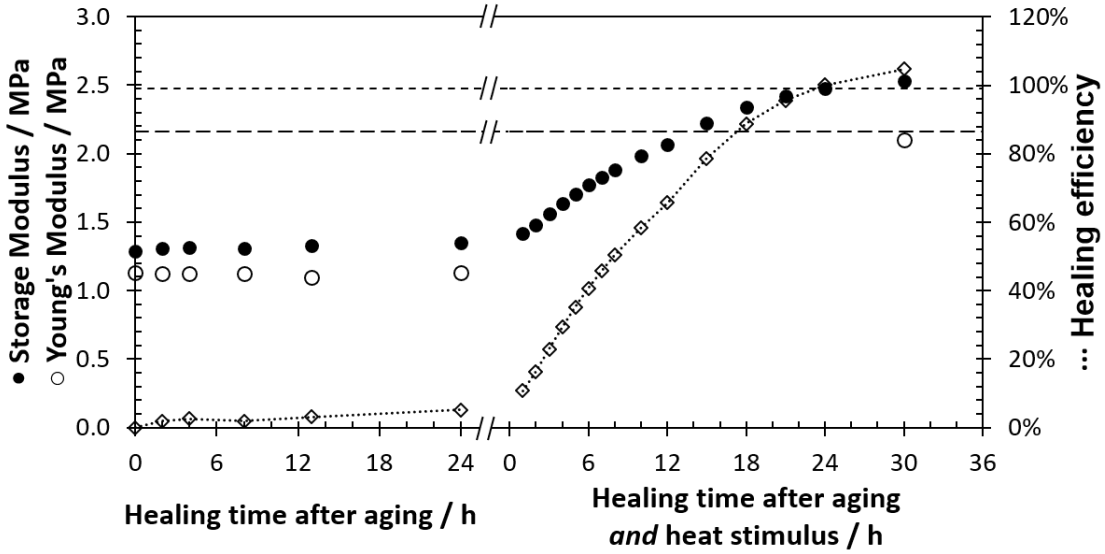

Figure 7 Storage modulus (solid markers, 1 Hz and 0.1 % strain) and Young's modulus (empty markers, 1 % strain and 0,1 MPa min^{-1}) of the damaged Sample 4 (damage surfaces aged for 12 h), compared to the original values prior to damage (horizontal short and long dashed lines, respectively). (left) Discontinuous measurements of modulus at 30 °C, showing no healing of aged damage surfaces. (right) Recovery of storage modulus, continuously monitored for 30 h at 30 °C, after heating to 80 °C for 4 h of aged damage surfaces. The healing efficiency (empty rhombii and dotted lines) is calculated using Equation 2.

~~*After* the heating step, the heat-treated damage surfaces were brought into contact again under minimal pressure and the sample was allowed to recover at 30 °C for several hours~~ The healing time of several hours at 30 °C is sufficient to shift the equilibrium back to the formation of the adduct bonds, thus reestablishing the mechanical properties of the network. Figure 7 (right) shows the evolution of the storage modulus (solid markers) and the Young's modulus (empty marker), after heating of the aged surfaces. After about 30 hours at 30 °C, both the storage and Young's moduli have recovered to the original values (dashed lines), resulting in healing efficiencies of 104.7 % and 94.5 %, respectively. Note that the exact time needed to recover properties will also depend on the quality of the surface contact (see requirement 3. of § 3.2.2) and on stress relaxation phenomena in the damage area of the heat-treated damage surfaces after closing the gap [36]. Experimental healing efficiencies slightly higher than 100 % could be explained by small differences in the cross-link density of the material due to minor differences in the environmental temperature, the residence time at that

temperature and resulting differences in the chemical equilibrium of the Diels-Alder reaction. In addition the relative error on the modulus determination in DMA is of the order of several %.

Both room-temperature healing and heating-mediated healing of the bulk samples in this work were performed at temperatures well below the de-gelation temperature of the ABMI400-F400 polymer network (de-gelation occurs between 90 °C and 115 °C [33]). The solid-like behavior in these conditions is important for both coating and structural applications to preserve the geometrical integrity of the material object while healing the incurred damage.

3.3.1 Microscopic evaluation of heating-mediated sealing of network coatings

Microscopy techniques are often used to monitor and visualize the formation of damage and subsequent sealing. Scanning Electron Microscopy [4,39,40], Atomic Force Microscopy [13] and optical microscopic techniques such as Laser Scanning Confocal Microscopy [41] are used for this task. In this work AFM and optical microscopy techniques are combined to provide information about the sealing of microscopic and macroscopic damage in F400-ABMI400 network coatings.

The nanolithography option of the AFM used in this work allows the application of user-defined patterns on a sample surface using a well-defined force, after the acquisition of the topography of the sample surface. This way, the surface of the sample can be damaged in a controlled and reproducible manner [13]. Scratches of about 5 µm long, a micrometer wide and close to half a micrometer deep are made in a 200 µm thick coating of the F400-ABMI400 reversible covalent polymer network (see line scans in Figure 8, top left, solid line).

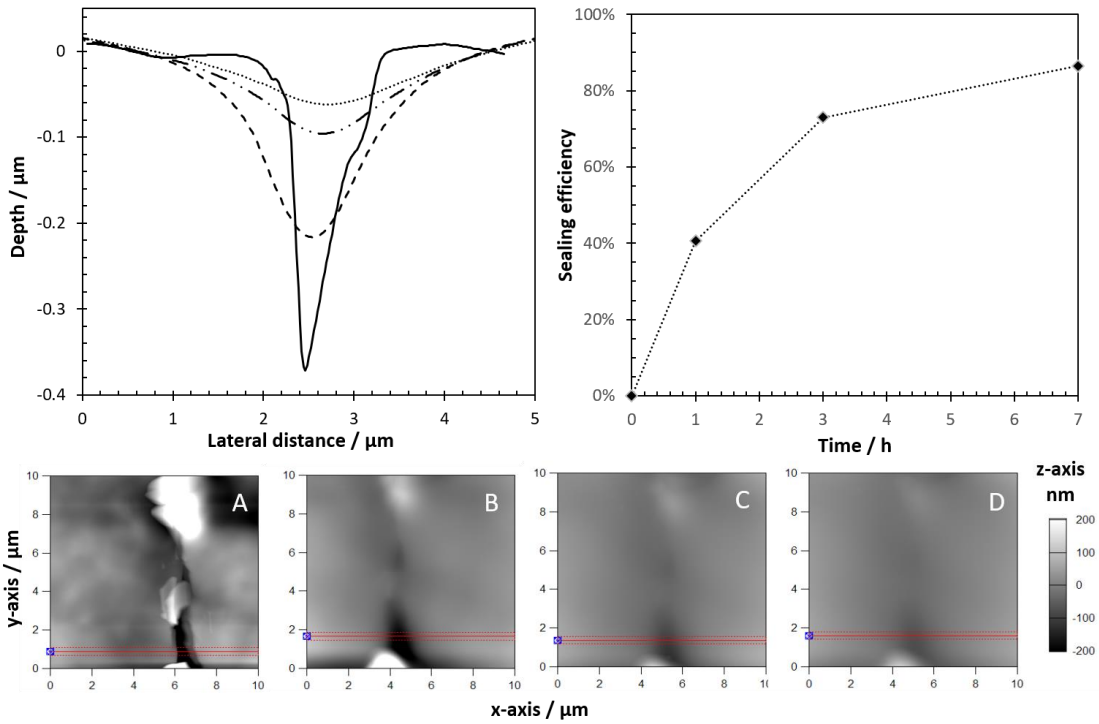

Figure 8 Depth profiles (top left) and sealing efficiency (top right) of the scratch in coating of F400-ABMI400 network made by nanolithography and assessed using Atomic Force Microscopy, as shown in the topography images (bottom) for the fresh scratch (A) and during sealing of the damage at 80 °C for (B) 1 h, (C) 3 h and (D) 7 h.

After the material was damaged the healing mechanism needs to be activated. In this first step of the self-healing process, the necessary mobility needs to be created to fill and seal the created damage volume. Using the in-situ heating stage, the damaged sample is heated to 80 ºC for 1 hour to induce the retro DA reaction. As the retro DA reaction proceeds furan and maleimide moieties become available and mobility is increased within the system. After the first heating step the sample was cooled to monitor the sealing effect at that stage (see Figure 8B). With only 1 hour at 80 ºC the depth of the damage has clearly decreased from 0.34 µm to 0.22 µm. Further heat treatment of two more hours at 80 °C leads to a bigger closure of the defect reducing the depth to less than 0.1 µm (Figure 8C). Heating the sample four hours more makes a further reduction of the defect to 0.05 µm, very close to the initial surface level. The AFM traces in Figure show how the surface of the sample changes during the whole process, showing that at the end of the thermal treatment the surface is almost as smooth as the non-damaged part. From the depth profiles, it can be noticed how upon heating the defect becomes wider and less deep, until it evens out with the rest of the material. The mobility gained by the network by heating to 80 °C was enough to fill a defect of this size. This is an important observation taking into account that at 80 °C the material still exhibits

solid-like behavior with network properties according to previous studies [33], meaning that sealing of this size of damages is possible without the need for the material to flow viscously, retaining the structural integrity of the coating.

In this stage the sealing step can be quantified as a 'sealing efficiency', η_{seal}, determined by the amount of damage volume that is sealed V_{sealed}, relative to the initial damage volume V_{damage}, given by Equation 5. This equation can be derived from the property recovery healing indicator (Equation 2), considering that the sealed volume V_{sealed} is equal to the initial damage volume $V(0)$ minus the damage volume $V(t)$ at a certain time t. The evolution of η_{seal} is shown in Figure (top right).

$$\eta_{\text{seal}} = \frac{V_{\text{sealed}}}{V_{\text{damage}}} = 1 - \frac{V(t)}{V(0)} \qquad \text{Equation 5}$$

As shown, the sealing ability of the studied thermally reversible network becomes more efficient and faster as the mobility increases at 80 ºC. This works very well for the µm-scale scratches as applied by nanolithography; however, if the damage becomes too big or too much material is removed from the damage area in the coating, the sealing step becomes more difficult.

Optical microscopy images in Figure 9 show the sealing of a scratch made in a 200 µm thick coating. This time the depth (200 µm) and width (125 µm) of the scratch are of about the same magnitude as the thickness of the coating itself (see Figure 9A). Using the same temperature treatment at 80 °C during 4 hours, as previously shown for the AFM lithography scratches, results in very little sealing of the wider scratch due to the large gap that needs to be covered (see Figure 9B). In the next step the sample was heated at 0.5 °C min^{-1} from 80 °C to 120 °C, following the Diels-Alder equilibrium [33], to determine the temperature at which the mobility of the sample was enough to seal the scratch. At 90 °C no significant further sealing was observed (see Figure 9C); however, at 100 °C the narrowest parts of the defect were sealed by a mechanism known as stitching (see Figure 9D).

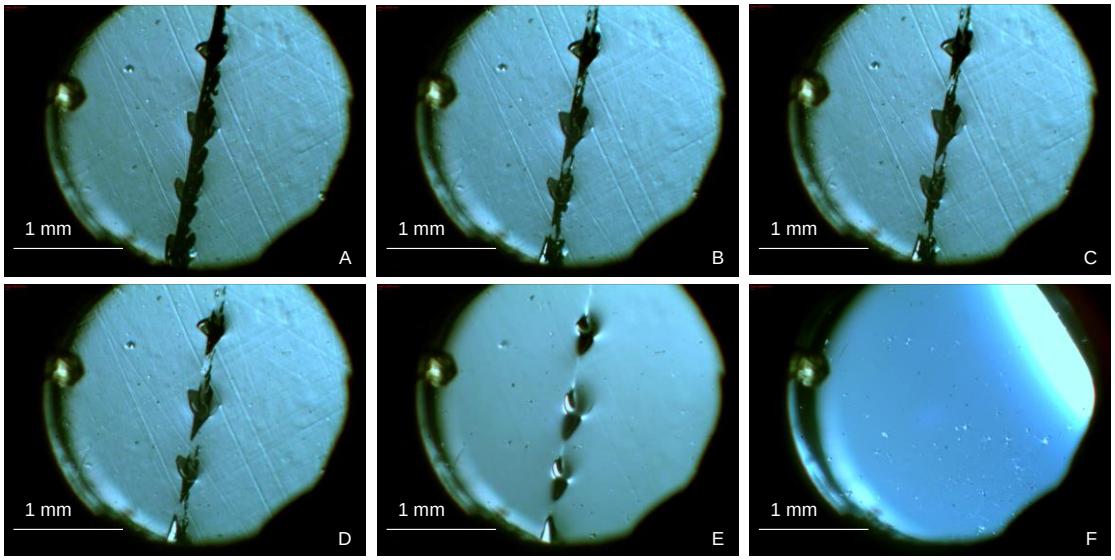

Figure 9 Optical microscopy images of the sealing of a 125 µm wide scratch in a 200 µm thick coating of F400-ABMI400 network: (A) the initial scratch; (B) 4 hours at 80 °C and subsequently heated at 0.5 °C min^{-1} to (C) 90 °C; (D) 100 °C; (E) 110 °C and (F) 120 °C.

From a temperature of 110 °C on, enough mobility is created to partially remove the applied damage volume, including the lines on the surface of the coating, caused by the production process of the coatings (see Figure 9E). This is consistent with the viscoelastic behavior of this F400-ABMI400 system. Increasing the temperature to 120 ºC even further allows complete filling of the damage volume, after the network has been broken down and the material starts to show viscous flow behavior [33].

The microscopic evaluation shows how damage is sealed by filling the created damage volume. As the defects in a coating are sealed, the functional properties of the coating, such as barrier protection against e.g. corrosion of the underlying substrate, are only completely recovered if the mechanical properties of the coating are restored to their original values. This will occur upon cooling, as the Diels-Alder adducts reform and equilibrium at room temperature is reached again.

3.3.2 Repeatability of thermal cycling in heating-mediated healing

The repeatability of mechanical breaking (see § 3.2.1) and thermal breaking of furan-maleimide Diels-Alder cycloadduct bonds is a key factor for the use in self-healing materials. The aim is to design self-healing materials that can heal multiple times and show full recovery of their functional properties after each healing cycle.

The thermal reversibility of the Diels-Alder reaction has been well-established. In bulk applications however the upper limit for the reversibility is a more pressing issue, as side

reactions of the maleimide functional group may take place at elevated temperatures (homopolymerization and Michael addition reaction) [42]. The thermal stability and repeatability of the bond breaking and reforming processes was studied using DSC. A sample of the F400-ABMI400 dynamic covalent polymer network system was subjected to thermal cycles of 10 min at 120 °C (long enough for the system to reach equilibrium at this temperature by breaking of the Diels-Alder bonds), followed by subsequent cooling to 50 °C to reform the broken bonds. During each isothermal segment at 50 °C the forward DA reaction (an exothermic process) of the network formation is monitored by DSC. Figure 10 shows the experimental heat flow signals of the 1st, 9th and 10th cycle during the isothermal reforming of the bonds at 50 °C. The heat flow during the bond formation process is proportional to the conversion rate of the Diels-Alder reaction (Equation 6), which in turn depends on the conversion $x(t)$, the initial concentration of the furan and/or maleimide functional groups and the rate constants for the forward and retro Diels-Alder reactions, k_{DA} and k_{rDA}, respectively, as shown in Equation 7 [33]. The heat flow signals after subsequent heating cycles lie consistently on top of each other. This is an indication that the conversion rate is still the same after multiple cycles, meaning that the reaction is still fully reversible after at least 10 thermal cycles between 120 °C and 50 °C. These experimental results are confronted with a simulation (dashed black line in Figure 10) based on the kinetic parameters of Table 1 [33], showing a good agreement between the experimental and simulated data.

$$\frac{\mathrm{d}Q(t)}{\mathrm{d}t} = \Delta_{\mathrm{r}}H^{\circ}\frac{\mathrm{d}x(t)}{\mathrm{d}t} \qquad \text{Equation 6}$$

$$\frac{\mathrm{d}x(t)}{\mathrm{d}t} = k_{\mathrm{DA}}[\mathrm{F}]_0(1-x(\mathrm{t}))^2 - k_{\mathrm{rDA}}x(t) \qquad \text{Equation 7}$$

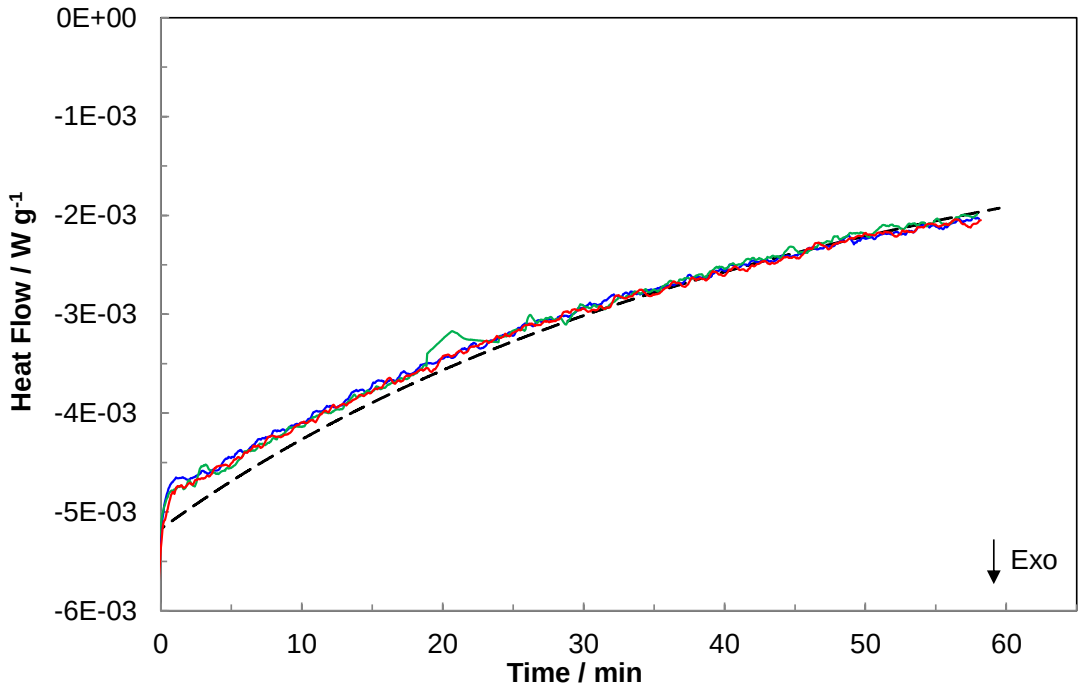

Figure 10 The experimental heat flow signals and a simulation of the heat flow during the reformation of the dynamic Diels-Alder bonds for the F400-ABMI400 polymer network under isothermal conditions at 50 °C after thermal dissociation at 120 °C; cycles 1 (green), 9 (red) and 10 (blue) are shown. Simulation according to kinetics of Table 1 [33] (black dashed line).

4. Conclusions

The ability to autonomously heal damage at room temperature was presented for the dynamically reversible covalent Diels-Alder network F400-AMBI400, provided that the damage surfaces are brought back into contact upon release of the damaging force. At room temperature rebonding of mechanically damaged surfaces was observed, when these surfaces are still fresh. In earlier work it was concluded from equilibrium thermodynamics that the Diels-Alder cycloadduct bonds are weaker than typical covalent bonds. It is thus concluded that these reversible bonds are broken preferentially when force is exerted onto the polymer chains, resulting in the formation of free furan and maleimide groups that are readily available to react and heal the damage as soon as the damage surfaces are brought back into contact. However, it took several days to recover the mechanical properties. The relaxation time defines the time necessary to return to equilibrium after a perturbation, such as the mechanical activation of the reversible bonds and consequently the time needed to recover the mechanical properties through new bond formation. It should be noted that stresses and topological network defects remain at the 'scar' of the original damage, resulting in earlier failure of the tested specimen. The remaining defects can still be healed and the resulting stresses can still relax over time by the dynamic nature of the reversible Diels-Alder bonds.

The required time at a certain temperature is determined by the cycloadduct lifetime, as existing bonds need to be broken and new bonds need to be formed.

It was shown that if the surfaces are kept apart and the equilibrium is allowed to reestablish (aging of the damage surfaces), healing did not occur during a comparable time frame. When the time to close the (mechanically activated) damage becomes of the order of the relaxation time of the equilibrium reaction, the excess furan and maleimide groups at the damage surfaces are consumed and no longer available to form new bonds across the surfaces to heal the damage. The healing potential of the damage surfaces can be replenished by the use of an external heat trigger. Using heating-mediated healing, the mechanical properties of the studied material first decrease overall due to the shift in equilibrium, breaking extra reversible covalent bonds, increasing the mobility of the polymer chains and speeding up the kinetics of the dynamically reversible reactions. Heating the material to 80 °C for 4 hours resulted in the sealing of the damage. After the sealing action, the mechanical properties were restored after 30 h at 30 °C, as the equilibrium shifts back to the formation of the bonds. The chosen temperature is well below the de-gelation point, meaning that the material can be healed using an external heat trigger without the loss of its geometrical and structural integrity.

In coatings of F400-AMBI400 crosslinked networks the self-healing at room temperature is not observed because adhesion of the coating to the substrate prevents making contact between the damage surfaces. Therefore heating-mediated healing is recommended for this type of applications. The use of visualization techniques in combination with techniques to evaluate the loss and recovery of functional properties is important to obtain a complete and thorough understanding of the underlying mechanisms of the healing action.
With microscopic techniques controlled damage applied to the surface of a coating could be quantified by the volume of the damage. It was observed, that for small defects a mild heating (T = 80 ºC) is enough to successfully seal the damage, preserving the network structure of the coating. For bigger damage, heating to elevated temperatures (T > 115 ºC) is necessary to destroy the network structure and make the material flow into the defect to seal it and close the gap between the damage surfaces. The efficiency of this step can be quantified as a ‘sealing efficiency’ that expresses how much of the original damage volume is sealed successfully.
It can be concluded that the F400-ABMI400 Diels-Alder crosslinked network in bulk can repair damage at room temperature due to a combination of: (i) the weaker strength of the reversible Diels-Alder bonds, considering that the formed σ bonds in the DA cycloadduct break in a concerted process to form furan (diene) and maleimide (dienophile) functionalities, (ii) the kinetics of the DA reaction of the F400-ABMI400 system, giving a dynamic character

to the reversible bonds which allows reasonable healing timescales, and (iii) the sufficient mobility of the polymer chains (the equilibrium F400-ABMI400 network has a glass transition T_g of about 3 °C at room temperature), resulting in a tough rubbery material at the reference temperature of 30 °C. This is an excellent compromise between the kinetics of the Diels-Alder reaction, the crosslink density and mechanical properties, and the value of T_g of the network just below application temperature. A value for T_g equal to or higher than the application temperature would result in a mobility-restricted system and drastically slow down the healing action in a thermoset network with higher crosslink density and increased modulus. A lower T_g for the same polymer chemistry would result in a lower crosslink density with decreased concentration of furan and maleimide groups, and slower healing in an elastomer network with decreased modulus.

Acknowledgements

M.M.D. gratefully acknowledges SIM (Strategic Initiative Materials in Flanders) in the framework of the SHE-NAPROM (SIM 2009-1, SBO 3) project for the financial support.

References

[1] S. Van Der Zwaag, Routes and mechanisms towards self healing behaviour in engineering materials, Bull. Polish Acad. Sci. 58 (2010) 227–236. doi:10.2478/v10175-010-0022-6.

[2] S. Van Der Zwaag, Self Healing Materials: An Alternative Approach to 20 Centuries of Materials Science, Springer, Dordrecht, The Netherlands, 2007.

[3] E.B. Murphy, F. Wudl, The world of smart healable materials, Prog. Polym. Sci. 35 (2010) 223–251. doi:10.1016/j.progpolymsci.2009.10.006.

[4] E. Brown, N.R. Sottos, S.R. White, Fracture Testing of a Self-Healing Polymer Composite, Exp. Mech. 42 (2002) 372–379. doi:10.1177/001448502321548193.

[5] E.N. Brown, S.R. White, N.R. Sottos, Microcapsule induced toughening in a self-healing polymer composite, J. Mater. Sci. 39 (2004) 1703–1710. doi:10.1023/B:JMSC.0000016173.73733.dc.

[6] B.J. Blaiszik, N.R. Sottos, S.R. White, Nanocapsules for self-healing materials, Compos. Sci. Technol. 68 (2008) 978–986. doi:10.1016/j.compscitech.2007.07.021.

[7] B.J. Blaiszik, S.L.B. Kramer, S.C. Olugebefola, J.S. Moore, N.R. Sottos, S.R. White, Self-healing polymers and composites, Annu. Rev. Mater. Res. 40 (2010) 179–211. doi:10.1146/annurev-matsci-070909-104532.

[8] R.S. Trask, I.P. Bond, Bioinspired engineering study of Plantae vascules for self-healing composite structures., J. R. Soc. Interface. 7 (2010) 921–31. doi:10.1098/rsif.2009.0420.

[9] K.S. Toohey, N.R. Sottos, J.A. Lewis, J.S. Moore, S.R. White, Self-healing materials with microvascular networks, Nat. Mater. 6 (2007) 581–585. doi:10.1038/nmat1934.

[10] H.R. Williams, R.S. Trask, I.P. Bond, Self-healing composite sandwich structures, Smart Mater. Struct. 16 (2007) 1198–1207. doi:10.1088/0964-1726/16/4/031.

[11] A. Torre-Muruzabal, L. Daelemans, G. Van Assche, K. De Clerck, H. Rahier, Creation of a nanovascular network by electrospun sacrificial nanofibers for self-healing applications and its effect on the flexural properties of the bulk material, Polym. Test. 54 (2016) 78–83. doi:10.1016/j.polymertesting.2016.06.026.

[12] D.Y. Wu, S. Meure, D. Solomon, Self-healing polymeric materials: A review of recent developments, Prog. Polym. Sci. 33 (2008) 479–522. doi:10.1016/j.progpolymsci.2008.02.001.

[13] J. Brancart, G. Scheltjens, T. Muselle, B. Van Mele, H. Terryn, G. Van Assche, Atomic force microscopy-based study of self-healing coatings based on reversible polymer network systems, J. Intell. Mater. Syst. Struct. 25 (2014) 40–46. doi:10.1177/1045389X12457100.

[14] D. Ratna, J. Karger-Kocsis, Recent advances in shape memory polymers and composites: A review, J. Mater. Sci. 43 (2008) 254–269. doi:10.1007/s10853-007-2176-7.

[15] H. Meng, G. Li, Feature article A review of stimuli-responsive shape memory polymer composites, Polymer. 54 (2013) 2199–2221. doi:10.1016/j.polymer.2013.02.023.

[16] S.R. White, J.S. Moore, N.R. Sottos, B.P. Krull, W.A.S. Cruz, R.C.R. Gergely, Restoration of Large Damage Volumes in Polymers, Science. 344 (2014) 620–623. doi:10.1126/science.1251135.

[17] S. Billiet, X.K.D. Hillewaere, R.F.A. Teixeira, F.E. Du Prez, Chemistry of Crosslinking Processes for Self-Healing Polymers, Self-Healing Polym. From Princ. to Appl. 34 (2013) 290–309.

[18] X.K.D. Hillewaere, F.E. Du Prez, Fifteen chemistries for autonomous external self-healing polymers and composites, Prog. Polym. Sci. 49–50 (2015) 121–153. doi:10.1016/j.progpolymsci.2015.04.004.

[19] D. Montarnal, M. Capelot, F. Tournilhac, L. Leibler, Silica-Like Malleable Materials from Permanent Organic Networks, Science. 334 (2011) 965–968. doi:10.1126/science.1212648.

[20] J.M. Lehn, Dynamers: Dynamic molecular and supramolecular polymers, Prog. Polym. Sci. 30 (2005) 814–831. doi:10.1071/CH10035.

[21] J. Canadell, H. Goossens, B. Klumperman, Self-healing materials based on disulfide links, Macromolecules. 44 (2011) 2536–2541. doi:10.1021/ma2001492.

[22] Y. Higaki, H. Otsuka, A. Takahara, A thermodynamic polymer cross-linking system

based on radically exchangeable covalent bonds, Macromolecules. 39 (2006) 2121–2125. doi:10.1021/ma052093g.

[23] C. Yuan, M.Z. Rong, M.Q. Zhang, Z.P. Zhang, Y.C. Yuan, Self-healing of polymers via synchronous covalent bond fission/radical recombination, Chem. Mater. 23 (2011) 5076–5081. doi:10.1021/cm202635w.

[24] J.F. Xu, Y.Z. Chen, L.Z. Wu, C.H. Tung, Q.Z. Yang, Dynamic covalent bond based on reversible photo [4 + 4] cycloaddition of anthracene for construction of double-dynamic polymers, Org. Lett. 15 (2013) 6148–6151. doi:10.1021/ol403015s.

[25] J. Van Damme, O. van den Berg, J. Brancart, L. Vlaminck, C. Huyck, G. Van Assche, B. Van Mele, F. Du Prez, Anthracene-Based Thiol–Ene Networks with Thermo-Degradable and Photo-Reversible Properties, Macromolecules. 50 (2017) 1930–1938. doi:10.1021/acs.macromol.6b02400.

[26] J.M. Craven, Cross-linked thermally reversible polymers produced from condensation polymers with pendant furan groups cross-linked with maleimides, US3435003, 1969.

[27] X. Chen, A Thermally Re-mendable Cross-Linked Polymeric Material, Science. 295 (2002) 1698–1702. doi:10.1126/science.1065879.

[28] Y.-L. Liu, Y.-J. Chen, W.-L. Wei, Novel thermosetting resins based on 4-(N-maleimidophenyl)glycidylether I. Preparation and characterization of monomer and cured resins, Polymer. 44 (2003) 6465–6473. doi:10.1016/j.polymer.2003.08.006.

[29] G. Scheltjens, M.M. Diaz, J. Brancart, G. Van Assche, B. Van Mele, A self-healing polymer network based on reversible covalent bonding, React. Funct. Polym. 73 (2013) 413–420. doi:10.1016/j.reactfunctpolym.2012.06.017.

[30] S. Terryn, G. Mathijssen, J. Brancart, D. Lefeber, G. Van Assche, B. Vanderborght, Development of a self-healing soft pneumatic actuator: a first concept, Bioinspir. Biomim. 10 (2015) 046007. doi:10.1088/1748-3190/10/4/046007.

[31] S. Terryn, G. Mathijssen, J. Brancart, T. Verstraten, G. Van Assche, B. Vanderborght, Toward Self-Healing Actuators: A Preliminary Concept, IEEE Trans. Robot. 32 (2016) 736–743. doi:10.1109/TRO.2016.2558201.

[32] S. Terryn, J. Brancart, D. Lefeber, G. Van Assche, B. Vanderborght, Self-healing soft pneumatic robots, Sci. Robot. 2 (2017) 1–12. doi:10.1126/scirobotics.aan4268.

[33] M.M. Diaz, G. Van Assche, F.H.J. Maurer, B. Van Mele, Thermophysical characterization of a reversible dynamic polymer network based on kinetics and equilibrium of an amorphous furan-maleimide Diels-Alder cycloaddition, Polymer. 120 (2017) 176–188. doi:10.1016/j.polymer.2017.05.058.

[34] D.G. Bekas, K. Tsirka, D. Baltzis, A.S. Paipetis, Self-healing materials: A review of advances in materials, evaluation, characterization and monitoring techniques, Compos. Part B Eng. 87 (2016) 92–119. doi:10.1016/j.compositesb.2015.09.057.

[35] G. Scheltjens, J. Brancart, I. De Graeve, B. Van Mele, H. Terryn, G. Van Assche, Self-healing property characterization of reversible thermoset coatings, J. Therm. Anal. Calorim. 105 (2011) 805–809. doi:10.1007/s10973-011-1381-4.

[36] X. Kuang, G. Liu, X. Dong, D. Wang, Correlation between stress relaxation dynamics and thermochemistry for covalent adaptive networks polymers, Mater. Chem. Front. 1 (2017) 111–118. doi:10.1039/C6QM00094K.

[37] F. Pilate, A. Toncheva, P. Dubois, J.M. Raquez, Shape-memory polymers for multiple applications in the materials world, Eur. Polym. J. 80 (2016) 268–294. doi:10.1016/j.eurpolymj.2016.05.004.

[38] V. Sessini, J.M. Raquez, G. Lo Re, R. Mincheva, J.M. Kenny, P. Dubois, L. Peponi, Multiresponsive Shape Memory Blends and Nanocomposites Based on Starch, ACS Appl. Mater. Interfaces. 8 (2016) 19197–19201. doi:10.1021/acsami.6b06618.

[39] S.R. White, N.R. Sottos, P.H. Geubelle, J.S. Moore, M.R. Kessler, S.R. Sriram, E.N. Brown, S. Viswanathan, Autonomic healing of polymer composites, Nature. 409 (2001) 794–797. doi:10.1038/35057232.

[40] R.J. Varley, S. Van der Zwaag, Towards an understanding of thermally activated self-healing of an ionomer system during ballistic penetration, Acta Mater. 56 (2008) 5737–5750. doi:10.1016/j.actamat.2008.08.008.

[41] Y. González-García, J.M.C. Mol, T. Muselle, I. De Graeve, G. Van Assche, G. Scheltjens, B. Van Mele, H. Terryn, A combined mechanical, microscopic and local electrochemical evaluation of self-healing properties of shape-memory polyurethane coatings, Electrochim. Acta. 56 (2011) 9619–9626. doi:10.1016/j.electacta.2011.03.081.

[42] A. V. Tungare, G.C. Martin, Analysis of the curing behavior of bismaleimide resins, J. Appl. Polym. Sci. 46 (1992) 1125–1135. doi:10.1002/app.1992.070460701.